Aerosol and Air Quality Research, 11: 487–496, 2011

ISSN: 1680-8584 print / 2071-1409 online
doi: 10.4209/aaqr.2011.05.0057

A Low Pressure Drop Preseparator for Elimination of Particles Larger than 450 nm

C. Asbach[1*], H. Fissan[1,2], H. Kaminski[1], T.A.J. Kuhlbusch[1,2], D.Y.H. Pui[3], H. Shin[3,4], H.G. Horn[5], T. Hase[6]

[1] *Institute of Energy and Environmental Technology (IUTA) e.V., 47229 Duisburg, Germany*
[2] *Center for Nanointegration Duisburg-Essen (CeNIDE), 47057 Duisburg*
[3] *University of Minnesota, Minneapolis, MN 55455, USA*
[4] *now at: KOTEC, Bukgu, Ulsan 68337, Korea*
[5] *TSI GmbH, 52068 Aachen, Germany*
[6] *TSI Inc., Shoreview, MN 55126, USA*

ABSTRACT

Measurement techniques which allow the detection of airborne nanoparticles are of great interest for e.g. exposure monitoring and quality control during nanoparticle production. An increasing number of commercial devices use a unipolar diffusion charger to charge the particles and determine the nanoparticle concentration and sometimes size. The analysis however may be biased by the presence of large particles. We therefore developed a preseparator that removes particles larger than 450 nm, i.e the minimum in the range of particle lung deposition curves, but only causes a low pressure drop. The preseparator uses a total flow rate of 2.5 L/min and consists of two stages. The first stage is a virtual impactor that removes particles larger than approximately 1 μm with a minor flow of 1 L/min. Particles above 450 nm are removed from the remaining 1.5 L/min in the cyclone of the second stage. The combination of a cyclone with a virtual impactor was shown to reduce the pressure drop of the preseparator from 8.1 to 5.6 kPa compared with a cyclone alone and improve the sharpness of the separation curve for cut-off diameters around 450 nm. Furthermore the virtual impactor extends the cleaning intervals of the preseparator, because large particles are no longer deposited in the cyclone. Eventually the preseparator was tested with an opposed flow diffusion charger and it was shown that particle charging is not affected by the pressure drop.

Keywords: Cyclone; Virtual impactor; Diffusion charger; Nanoparticle.

INTRODUCTION

Nanoparticles, here synonymously also used for nanoplates and nanofibres, can be considered as important building blocks for nanostructured materials. There is concern that these engineered nanoparticles can be released into the environmental media air, water and soil, during their entire lifecycle, i.e. during synthesis, handling, downstream use or recycling (Mueller and Nowack, 2008; Som *et al*., 2010). This may lead to exposure of human beings and the ecosystem with corresponding possible risks (Borm *et al*., 2006; Warheit *et al*., 2008). Inhalation is currently seen as the most important route of nanomaterial intake by humans (Oberdörster, 2010).

Online exposure related measurements of nanoparticle concentrations in air as well as off-line analysis of nanoparticle properties after sampling on a substrate may be biased by larger particles and nanoscale particles from other sources. An increasing number of direct-reading instruments for the detection of nanoparticles use electrical sensors due to their ease of use, low power consumption and small size. Such electrical sensors normally comprise a corona discharge to produce unipolar ions, a chamber for diffusive ion attachment to the aerosol particles (Hernandez- Sierra *et al*., 2003; Park *et al*., 2007) followed by an ion trap to remove excess ions. The particles are eventually collected e.g. on an absolute filter and the particle induced current is measured with a Faraday cup electrometer (Fissan *et al*., 2007; Marra *et al*., 2010; Fierz *et al*., 2011). These diffusion charger based electrical sensors are commonly used to infer total concentrations (number, length, active or lung deposited surface area) from the measured current. To do so, the average charge per particle has to follow the same size dependence as the wanted particle quantity. According to Fuchs' theory (Fuchs, 1963), however, the average charge level is proportional to the particle diameter squared in the free molecule regime and directly proportional to the

* Corresponding author. Tel.: +49 (0)2065 418-209;
Fax: +49 (0)2065 418-211
E-mail address: asbach@iuta.de

particle diameter in the continuum regime. In-between, the exponent of the diameter dependence gradually changes from one to two. Only in limited particle size ranges, the dependence can be approximated by power laws with constant exponents (Jung and Kittelson, 2005). Hence the particle size range of the test aerosols that are delivered to the diffusion charger has to be limited. It was shown for the Nanoparticle Surface Area Monitor (NSAM, TSI model 3550) that the device only delivers accurate estimates of the lung deposited surface area in a size range of approximately 20–400 nm (Asbach *et al*., 2009), because the lung deposition curves show a minimum around 300–500 nm. While the lower end of this size range is usually not critical due to the commonly negligible contribution of sub-20 nm particles to the total surface area concentration, the upper end has to be well adjusted by the use of an appropriate preseparator that removes all particles larger than 450 nm. In order not to bias the charging efficiency and not to overburden the pump, the pressure drop has to be kept as low as possible. Especially in view of future developments of portable or personal, battery-operated measurement devices, a low pressure drop is also crucial to keep the energy consumption low.

If an electrical mobility classification device is used between the diffusion charger and the electrometer to determine particle size distributions, an appropriate preseparator is also essential. On the one hand, like in an SMPS, the upper size limit has to be well known in order for the multiple charge correction to work properly (Hoppel, 1978; Fissan *et al*., 1983). On the other hand the electrical mobility of diffusion charged particles is becoming increasingly insensitive to particle diameter when approaching the continuum regime, because the Cunningham slip correction factor approaches unity and the charge level gets proportional to particle diameter. The measured mobility spectrum of particles larger than approximately 450 nm can hence not unambiguously be deconvoluted into a size distribution. In addition, as mentioned above, the lung deposition curves show a minimum around 300–500 nm. A preseparator with 450 nm cut-off hence allows for the measurement of particles that would diffusively deposit in the human airways.

We currently develop a portable, battery operated instrument that uses the abovementioned electrical sensor to measure total particle number and particle size-weighted concentrations. An electrical mobility classifier can be used as an optional module between charger and detector to measure size distributions. This paper describes the development and evaluation of a preseparator with a 450 nm cut-off and low pressure drop for this modular system, which operates at a total flow rate of 2.5 L/min. It is designed such that it can also be used for other diffusion charger based instruments, particularly NSAM (TSI, model 3550) or the largely identical TSI Aerotrak 9000. The preseparator is kept as small as possible so that it can be easily used in portable or personal instruments.

DESIGN OF PRESEPARATOR

The removal of large particles from an air stream is commonly achieved by inertial separation. The air stream is diverted from its straight path such that particles with high inertia cannot follow the streamlines. In an impactor, the flow is accelerated in a nozzle and directed towards a perpendicular impaction plate on which large particles are consequently deposited (Hinds, 1999). Impactors achieve sharp cut-off curves that can be predicted based on similitude by the flow velocity, the distance between nozzle outlet and impaction plate as well as nozzle size and shape. In a cyclone, the air flow is first accelerated in a nozzle and then exhibits a spiral shape inside a cylindrical or conical container and particles above certain inertia are deposited on the container walls. Cyclones have the advantage that they usually create a lower pressure drop than impactors for the same cut-off and particle re-entrainment from the collection surfaces is lower. The downside of cyclones is that there is no complete similitude concept to predict their separation characteristics. Instead their design is usually based on empirical models (Chan and Lippmann, 1977) or similarity with existing cyclones with known behaviour (Kenny and Gussman, 1997, 2000). Another way of estimating the separation efficiency of a cyclone is by the use of a model equation by Lapple (Lapple, 1951):

$$d_{p,50} = 3 \cdot \sqrt{\frac{\mu \cdot b}{2\pi \cdot \rho_p \cdot v_i \cdot N_e}} \quad (1)$$

where μ is the gas viscosity, b is the inlet diameter, ρ_p is the particle density, v_i is the gas inlet velocity and N_e is the number of effective turns the gas makes in the cyclone, with values commonly between 0.5 and 10 (Leith and Metha, 1973). Since N_e is usually unknown beforehand, Eq. (1) can only be used for a rough estimate.

In a virtual impactor, the total incoming flow is split into a major flow and a minor flow. The major flow is diverted by 90° whereas the minor flow is usually aligned with the aerosol inlet (Marple, 1980). Smaller particles follow the major flow streamlines, whereas particles with high inertia deviate from the major flow streamlines and are collected in the minor flow. Virtual impactors usually have a lower pressure drop than impactors or cyclones but also usually a less steep separation curve. They are often used for the concentration of large particles in the minor flow (e.g. Liebhaber *et al*., 1991; Sioutas *et al*., 1994).

The idea for the present preseparator was to combine the positive effects of a virtual impactor (low pressure drop) and a cyclone (steep separation curve) as illustrated in Fig. 1. In the first stage, particles larger than approximately 1 µm are removed from the sample stream in a virtual impactor. In the second stage, all remaining particles larger than the desired cut-off are removed in a cyclone. The total flow rate of the preseparator is 2.5 L/min, which is the intended flow rate of our portable instrument that uses an opposed flow diffusion charger (Medved *et al*., 2000), similar to the one used in TSI instruments NSAM (model 3550), Aerotrak 9000 and EAD (model 3070A). The virtual impactor has a minor flow of 1 L/min and a major flow of 1.5 L/min to match the two flow rates required by the charger (see Fig. 2). The charger uses 1.5 L/min aerosol

flow and a 1 L/min ion jet flow to convectively transport ions into the mixing chamber. The preseparator hence includes the flow splitter that is necessary for this particular type of charger. The cyclone in the second step is hence operated with the flow rate of 1.5 L/min. It was expected that the combination of virtual impactor with a cyclone can reduce the pressure drop across the preseparator while providing a cut-off diameter in the desired size range. Another advantage of the virtual impactor upstream is that no large particles are deposited in the cyclone, thus extending the necessary cleaning intervals.

Since there is no complete model for the design of cyclones, the NSAM/EAD cyclone was used as a starting point. This cyclone was designed according to Kenny and Gussman (2000) and operates at a total flow rate of 2.5 L/min with a cut-off diameter of 1.0 µm. The total flow rate is tangentially introduced through a 2.1 mm (0.083 in) nozzle into a cylindrical main body with a diameter of 8.8 mm (0.348 in) and a depth of 11.6 mm (0.457 in). The new preseparator was designed to be similar to this cyclone but including the first virtual impactor stage. The inlet nozzle is exchangeable, because the inlet flow velocity plays a crucial role in the performance of both, the virtual impactor and the cyclone, but its impact cannot be theoretically described due to the lack of a suitable theory. Therefore four different inlet nozzles were tested with diameters of 0.70 mm, 0.85 mm, 1.0 mm and 1.2 mm. The outlet nozzle for the minor flow of the virtual impactor has a diameter of 1.016 mm, but can alternatively be plugged. In the latter case, the preseparator acts as a cyclone and can be used

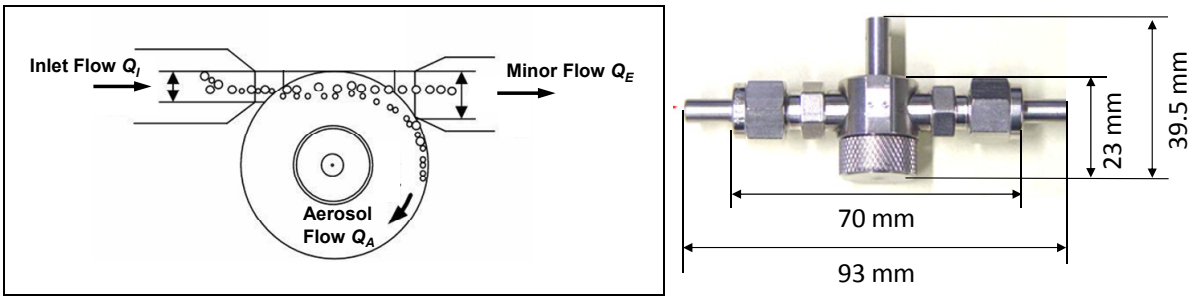

Fig. 1. Schematic and photograph of the preseparator.

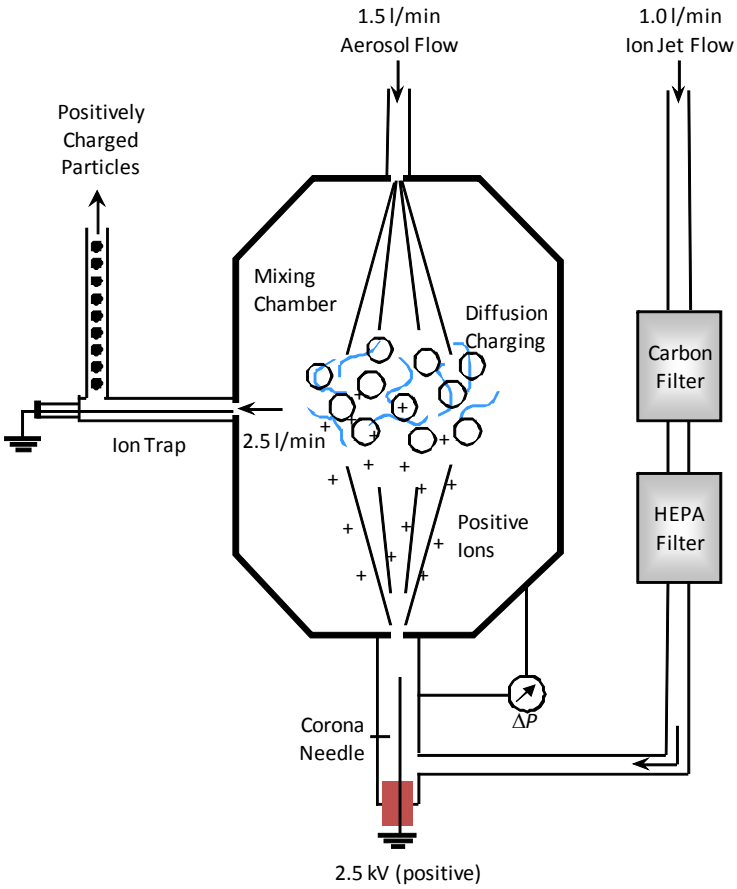

Fig. 2. Schematic of investigated unipolar diffusion charger (Medved *et al.*, 2000).

either with 1.5 L/min or 2.5 L/min aerosol flow, although a flow rate of 1.5 L/min is recommended due to the small dimensions of the cyclone body. The cylindrical main body of the cyclone has a diameter of 5.2 mm (0.205 in) and a depth of 6.17 mm (0.243 in). The overall outer dimensions of the preseparator are 93 mm × 39.5 mm (see Fig. 1)

PERFORMANCE MEASUREMENTS OF PRESEPARATOR

Initial measurements were conducted with a polydisperse aerosol to test the general performance concerning separation efficiency and pressure drop in different configurations of flow rates and nozzle diameters. Barium sulphate ($BaSO_4$) powder was suspended in DI water, sonicated and then aerosolized with an atomizer (TSI Tri Jet 3460) followed by a Nafion diffusion dryer (see Fig. 3). The BaSO4 powder originates from a grinding process. The effective particle density is hence identical with the bulk material density of 4500 kg/m³. Downstream of the dryer, the aerosol was neutralized with an ^{85}Kr Neutralizer (TSI model 3077) to avoid electrostatic particle losses in the sampling tubes and test cyclone. A glass compensation tank was used to match the flow rate of the atomizer of approximately 5 L/min with the inlet flow rate of the preseparator, i.e. 2.5 L/min or 1.5 L/min, respectively, depending on settings. The aerosol was then either fed through the test cyclone to measure the number size distribution downstream or the cyclone was bypassed to measure number size distributions upstream of the cyclone. Size distributions were measured with an SMPS (TSI model 3936-L86) with long DMA and an ultrafine water condensation particle counter. The minor flow and aerosol flow from the cyclone were maintained with needle valves and frequently checked with mass flow meters (TSI model 4140). The flow rates downstream of the cyclone were adjusted based on ambient pressure as requested by most instruments, e.g. NSAM or EAD, thus maintaining a constant (operating) flow rate of 2.5 L/min at the cyclone inlet. The pressure level downstream of the cyclone is slightly reduced because of its pressure drop, leading to slightly higher flow rates at operating pressure than 1.5 L/min and 1.0 L/min, respectively. Pressure levels and temperatures were measured in the respective flows and corrected as follows:

$$Q_{ambient} = Q_{operating} \cdot \frac{p_{operating}}{p_{ambient}} \cdot \frac{T_{ambient}}{T_{operating}} \quad (2)$$

where Q is flow rate, p is pressure and T is temperature. Concentrations, measured with a CPC were also corrected accordingly, since the CPC delivered the concentration always for operating pressure:

$$C_{N,ambient} = C_{N,operating} \cdot \frac{p_{ambient}}{p_{operating}} \quad (3)$$

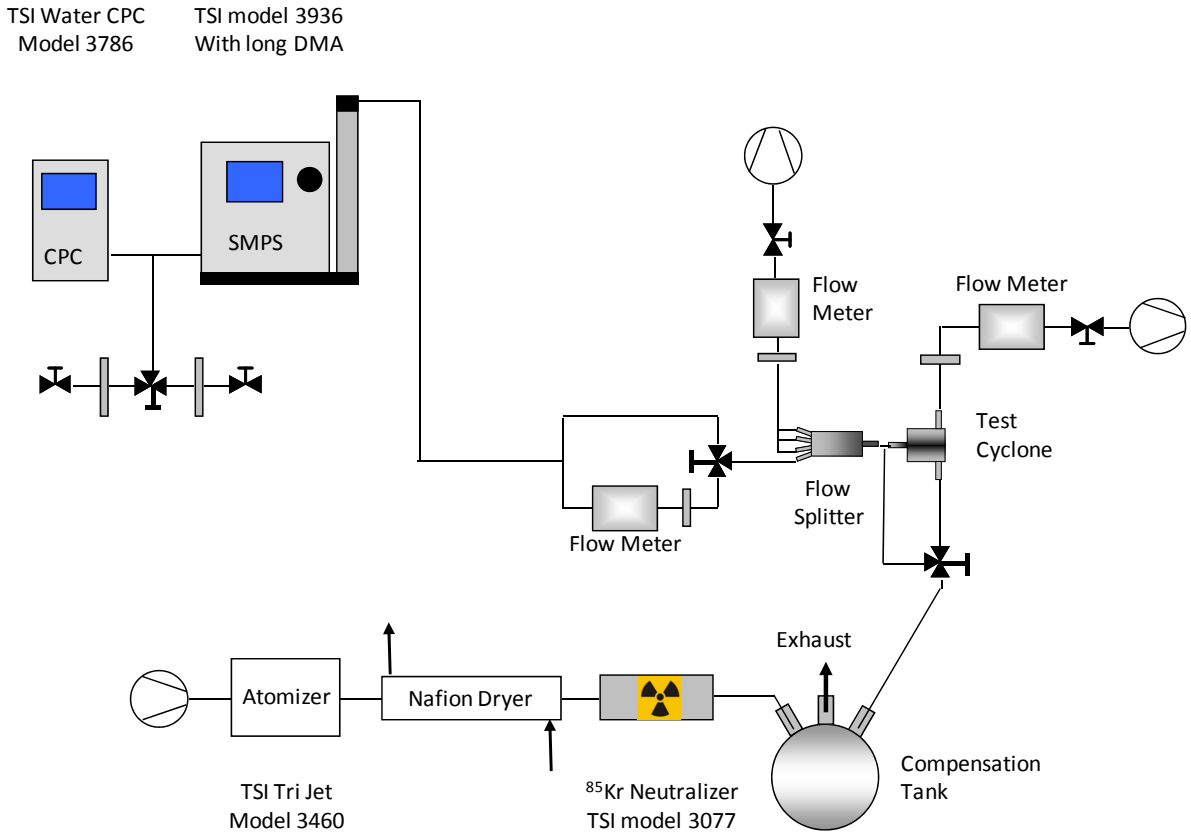

Fig. 3. Experimental set up for measurement of separation efficiency.

with number concentration C_N at ambient and operation conditions, respectively.

Ten separation efficiency curves were determined for each test series (four nozzles each with two flow rates). Each efficiency curve is constructed of the separation efficiencies from the 97 size bins of the SMPS. The separation efficiency η was determined according to:

$$\eta_{n,j} = 1 - \frac{C_{N,n,downstream}}{C_{N,n,upstream}} = 1 - \frac{2 \cdot C_{N,n,i}}{C_{N,n,(i-1)} + C_{N,n,(i+1)}} \quad (4)$$

where n is the running index for the particle size class (depending on the size range and size resolution of the SMPS, here ($1 \leq n \leq 97$), j is a running index for the individual separation efficiency measurement ($1 \leq j \leq 10$), and i is a running index for the individual size distribution measurements with $i = 2 \times j$. A mean separation efficiency curve was calculated by averaging the results for each of the particle size classes of the efficiency curves.

Results from the measurements with polydisperse particles with 1.5 L/min aerosol flow and 1.0 L/min minor flow are depicted in Fig. 4 for all four different inlet nozzle diameters. It can be clearly seen that a smaller inlet nozzle diameter decreases the cut-off diameter $d_{p,50}$ of the preseparator, however, the steepness of the separation curve is decreased. Furthermore the pressure drop is significantly affected by the nozzle diameter. While the pressure drop is only 3.5 kPa at $d_{p,50}$ of 490 nm with the largest nozzle (1.2 mm dia.) it is increased to more than 20 kPa at $d_{p,50}$ of 220 nm and 0.7 mm dia. nozzle.

Fig. 5 shows the separation efficiency measured with the minor flow outlet plugged and a total flow rate of 1.5 L/min. The preseparator was hence operated as a regular cyclone. The behaviour is generally comparable with the one shown in Fig. 4, i.e. decreasing $d_{p,50}$ and increasing pressure drop with decreasing nozzle diameter. Cut-off diameters, however, are between 451 nm with 0.7 mm nozzle and 742 nm with the 1.2 mm nozzle and thus significantly larger than during operation as a combined virtual impactor/cyclone. The combination of virtual impactor and cyclone furthermore shows a lower pressure drop at comparable cut off sizes (5.5 kPa and 439 nm cut-off with the combination compared with 8.1 kPa and 451 nm cut-off with the cyclone), proving the superior performance of the combination of virtual impactor and cyclone over the cyclone alone. Overall performance data are listed in Table 1. The table also gives values for the number of effective turns and corresponding cut off sizes, calculated with the Lapple Eq. (1). The effective number of turns the gas makes in the cyclone is between 5.1 and 9.7 for the different inlet nozzles and hence within the expected range $0.5 \leq N_E \leq 10$ (Leith and Mehta, 1973).

The requirement for the preseparator was to show a cut-off diameter of approximately 450 nm with an as-low-as-possible pressure drop. Based on the measurements with polydisperse particles, an inlet diameter of 1.0 mm was chosen for the combination of cyclone and virtual impactor. In this combination, the preseparator provides a cut-off diameter of 439 nm and a pressure drop of 5.5 kPa. To verify these data, measurements were repeated for this combination with certified polystyrene latex (PSL) particles (BS-Partikel, Wiesbaden, Germany). The experimental set up was identical with the one previously used for measurements with polydisperse particles (see Fig. 3). Five different particle sizes were investigated: 182 nm ± 5 nm, 305 nm ± 6 nm, 399 nm ± 8 nm, 522 nm ± 8 nm, and 726 nm ± 16 nm. The PSL particles came in liquid suspensions that were then further suspended in de-ionized water and sonicated. Number size distributions were alternately measured upstream and downstream of the cyclone. The separation efficiencies η were calculated according to Eq. (4) for every size bin. Fig. 6 indicates that

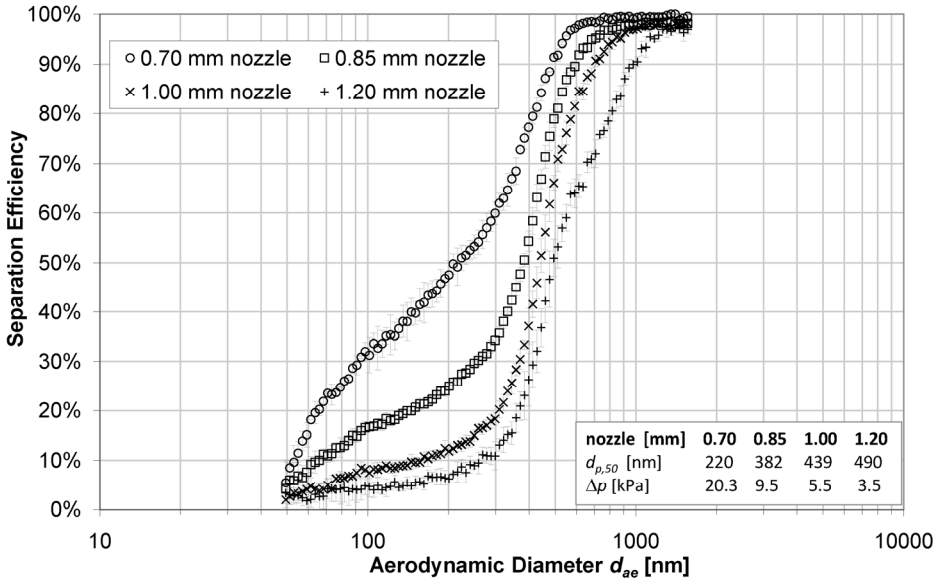

Fig. 4. Separation efficiency of preseparator with 1.5 L/min aerosol flow and 1.0 L/min minor flow, i.e. 2.5 L/min total flow with four different inlet nozzle diameters (0.7 mm, 0.85 mm, 1.0 mm, and 1.2 mm).

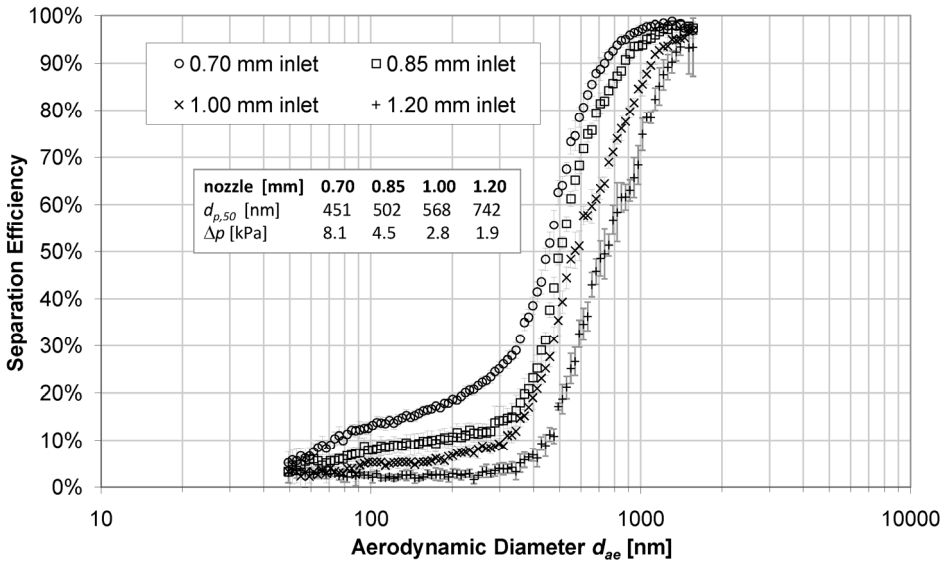

Fig. 5. Separation efficiency of preseparator in cyclone mode, i.e. with 1.5 L/min aerosol flow and plugged minor flow outlet; four different inlet nozzle diameters: 0.7 mm, 0.85 mm, 1.0 mm, and 1.2 mm

Table 1. Performance data of the combination of virtual impactor and cyclone (Q_A = 1.5 L/min, Q_m = 1.0 L/min) and "classic" cyclone (Q_A = 1.5 L/min, Q_m = 0 L/min) with four different inlet diameters; measured with polydisperse $BaSO_4$ particles; Lapple data according to Eq. (1).

lnlet dia. [mm]	0.70		0.85		1.00		1.20	
Setting	Q_A = 1.5 L/min Q_m = 1.0 L/min	Q_A = 1.5 L/min Q_m = 1.0 L/min	Q_A = 1.5 L/min Q_m = 1.0 L/min	Q_A = 1.5 L/min Q_m = 1.0 L/min	Q_A = 1.5 L/min Q_m = 1.0 L/min	Q_A = 1.5 L/min Q_m = 1.0 L/min	Q_A = 1.5 L/min Q_m = 1.0 L/min	Q_A = 1.5 L/min Q_m = 1.0 L/min
Δp [kPa]	20.3	8.1	9.5	4.5	5.5	2.8	3.5	1.9
$d_{p,50}$ [nm]	220	451	382	50	439	568	490	742
p_{amb} [kPa]	100.0	99.9	98.4	99.7	98.5	99.5	99.7	99.6
T_{amb} [°C]	26.8	26.8	27.9	27.9	26.4	26.8	27.7	27.7
$d_{p,50}$ Lapple	n/a	455.0	n/a	502.0	n/a	566.2	n/a	740.5
N_E Lapple	n/a	5.1	n/a	7.5	n/a	9.6	n/a	9.7

the results with PSL particles are very comparable with those obtained with $BaSO_4$ for the same cyclone settings. In Fig. 6, error bars indicate the standard deviations from the determination of the separation efficiency. The cut-off diameter was determined from a polynomial fit to be 455 nm and the measured pressure drop 5.6 kPa ± 0.14 kPa, compared with 439 nm and 5.5 kPa with $BaSO_4$.

The sharpness of the separation curve was calculated with the particle diameter at separation efficiencies of 16% and 84%

$$\text{Sharpness}=\sqrt{\frac{d_{84}}{d_{16}}} \quad (5)$$

The sharpness of the separation curve is 1.51 according to Eq. (4) with the d_{16} and d_{84} derived from the polynomial fit. The sharpness measured with $BaSO_4$ with the same cyclone settings was 1.54.

The pressure drop caused by the preseparator is fairly low with 5.6 kPa, which can be overcome by common pumps.

EFFECT OF PRESSURE DROP ON THE PERFORMANCE OF A DIFFUSION CHARGER

Besides pump limitations, a changed pressure may also affect the measurement principle in a downstream instrument, e.g. the charging efficiency in a diffusion charger. Several devices have recently been introduced that use unipolar diffusion charging to monitor the number or surface area concentration, including Electrical Aerosol Detector (TSI EAD model 3070A), Nanoparticle Surface Area Monitor (TSI NSAM model 3550) and Aerotrak 9000 (Fissan *et al*., 2007; Shin *et al*., 2007), Diffusion Size Classifier (Matter Engineering DiSC; Fierz, *et al*., 2002), Miniature Diffusion Size Classifier (Fierz *et al*., 2011), NanoTracer (Philips Aerasense, Marra, *et al*., 2010) and NanoCheck (Grimm Aerosoltechnik). In all these devices, particles are charged in a unipolar diffusion charger to an assumed particle size dependent average charge level. Ions are removed in an ion trap and finally the current induced by the charged particles upon deposition is measured. In order to infer a particle concentration from the current, the mean charge

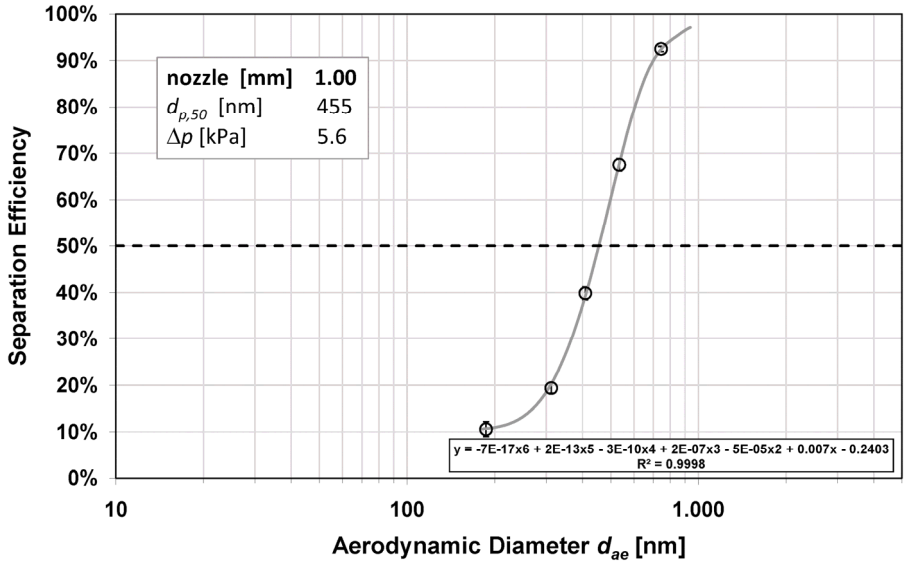

Fig. 6. Separation curve of the combination of cyclone with virtual impactor with NIST traceable polystyrene latex particles with 1.5 L/min aerosol flow, 1.0 L/min minor flow and 1.0 mm inlet nozzle.

per particle has to be known. In general, the average charge per particle n_c can be estimated as follows (Hinds, 1999):

$$n_c = \frac{2\pi \cdot \varepsilon_0 \cdot d_p \cdot k \cdot T}{e^2} \cdot \ln\left(1 + \frac{d_p \cdot \bar{u}_{t,i} \cdot e^2 \cdot n_i \cdot t}{8 \cdot \varepsilon_0 \cdot k \cdot T}\right) \quad (6)$$

In Eq. (6) ε_0 is the dielectric constant (8.854×10^{-12} AsV/m), d_p is the particle diameter, k is the Boltzmann constant (1.381×10^{-23} J/K), T is the absolute temperature, e is the elementary charge (1.602×10^{-19} As), $\bar{u}_{t,i}$ is the mean thermal speed of ions, n_i is the ion concentration and t is the residence time of particles in the ion atmosphere. In Eq. (6) ion concentration and residence time may be pressure dependent. Since these parameters are neither easily theoretically predictable nor directly experimentally accessible, experiments were conducted to measure the particle charging efficiency of an opposed flow unipolar diffusion charger with and without a simulated pressure drop of the preseparator. The charger, shown in Fig. 2, is used in three commercial instruments by TSI (EAD model 3070A, NSAM model 3550 and Aerotrak 9000) and very similar to the one used in our modular system under development. The charger uses two flows, an aerosol flow of 1.5 L/min and an ion jet flow of 1.0 L/min. The aerosol is directly transported into a mixing chamber, while the ion jet flow is first completely filtered, before it passes a corona needle and then convectively transports ions from the corona into the mixing chamber. The mixing chamber is free of any electrical fields. Ions and particles therefore only collide due to diffusion (Medved *et al*., 2000). Downstream of the mixing chamber, ions are removed from the aerosol flow in an electrostatic ion trap. The ion trap is a coaxial arrangement with the aerosol flowing between inner and outer electrode. When a low voltage is applied between the two electrodes, ions are electrostatically removed because of their high electrical mobility. This combination of charger and ion trap has been used in various studies in the past to investigate the charging efficiency (Jung and Kittelson, 2005), its correlation with surface area concentrations deposited in the human respiratory tract (Fissan *et al*., 2007; Shin *et al*., 2007; Wilson *et al*., 2007; Asbach *et al*., 2009), or the effect of pre-existing charges on the charging efficiency (Qi *et al*., 2007).

During the experiments, the charger was maintained at 1.5 L/min aerosol flow and 1 L/min ion flow at atmospheric pressure, therefore the operation flow rate in the charger increases and hence the residence time decreases, when the pressure in the charger is reduced by the preseparator. In Eq. (6) ion concentration and residence time decrease with decreasing pressure assuming that the mass flow rate through the charger and the fraction of gas molecules that get ionized remain constant. However, since the pressure dependences are logarithmized, it was expected that the effect of the preseparator pressure drop on the charging efficiency is small.

Measurements were conducted to verify this assumption. The experimental set up is shown in Fig. 7. Either monodisperse PSL or polydisperse sodium chloride particles were generated using an atomizer (TSI Tri Jet, model 3460). Particles were dried with an internal dryer of the atomizer and an additional silica gel dryer (TSI, model 3062). To match the flow rate produced by the atomizer with the flow rate needed for the following classification and measurement, the aerosol was led through a compensation tank. For investigation of the charging efficiency with highly monodisperse particles, the aerosol was then size classified using a differential mobility analyzer (TSI long DMA, model 3081) following an ^{85}Kr neutralizer (TSI, model 3077A). The DMA was operated with a negative voltage to select only positively charged particles. Particles were again neutralized downstream of the DMA to bring particles to a charge equilibrium, because Qi *et al*. (2007)

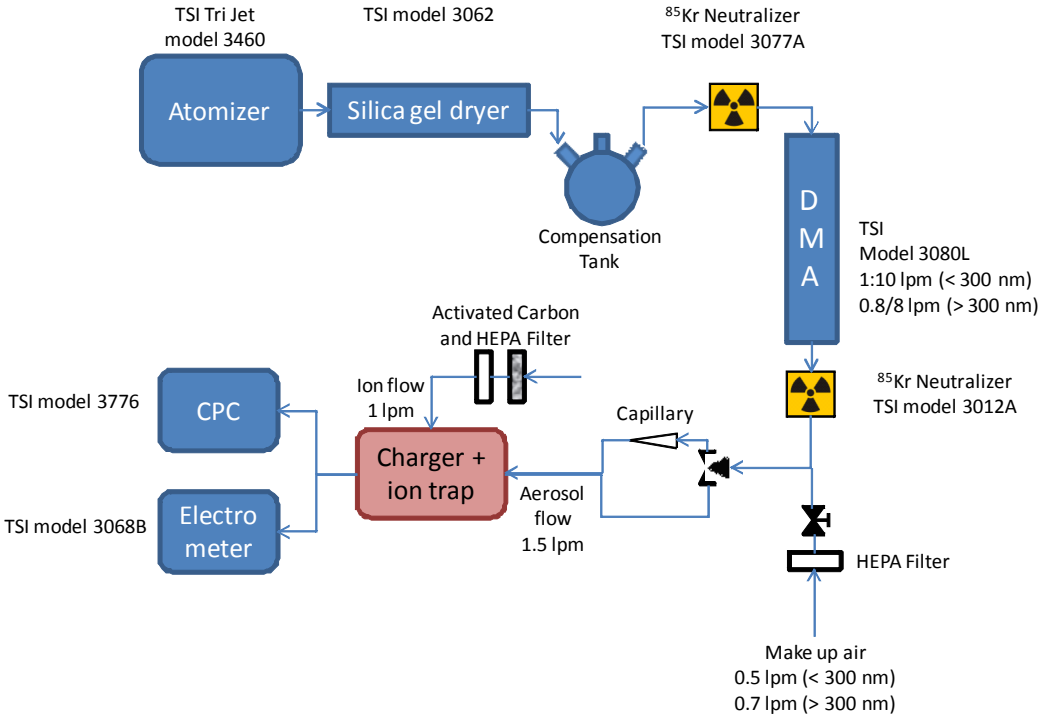

Fig. 7. Experimental set up for the measurement of pressure dependent charging efficiency.

have reported that a pre-charged aerosol of same polarity may acquire a higher charge level than neutralized particles. The aerosol was then passed through the charger, followed by the ion trap, operated at 20 V. The charger was maintained at its default settings, i.e. a corona voltage of approximately 2.5 kV with the corona current limited to 1 µA. Number concentration and total current provided by the particles were measured in parallel downstream of the charger/ion trap unit with a condensation particle counter (TSI model 3776) and an aerosol electrometer (TSI model 3068B). The mean charge per particle was then calculated as follows:

$$n_c = \frac{1}{Q_{el} \cdot C_N \cdot e} \tag{7}$$

where I is the total current measured by the electrometer, Q_{el} the flow rate through the electrometer, e the elementary charge and C_N the particle number concentration measured with the CPC. The effect of a pressure drop upstream of the charger was simulated by adding a capillary between DMA and charger. The preseparator could not be used with the NSAM charger as it is, because the charger flow rates are controlled by means of critical orifices in the charger block. Since the minor and major flow outlets of the preseparator have slightly different pressure levels, the required flow ratio in the charger could not be maintained without changing the orifices.

As a first step, the charging efficiency was measured without an additional pressure drop upstream and compared with literature data from Jung and Kittelson (2005) and data from the data sheet of the Electrical Aerosol Detector. In the present study, particle sizes of 50, 80, 100, 150, and 200 nm were classified from a polydisperse NaCl Aerosol. 246 nm particles were additionally produced from a polystyrene latex (PSL) suspension. Results are shown in Fig. 8. The gas pressure was measured downstream of the charger with the internal pressure gauge of the CPC. Since the charger flows are maintained by orifices, the pressure inside the charger is always lower than ambient pressure. Pressure levels of 96.3 kPa and 95.5 kPa in Fig. 8 hence refer to measurements without artificial pressure drop. The "atmospheric" pressure levels are slightly different, because measurements were performed on two different days. Jung and Kittelson (2005) and TSI presented equations that fit their mean charge levels. Jung and Kittelson investigated the charging efficiency in a size range of 30–150 nm, TSI (2004) from 10 to 400 nm. The graphs of both equations are given in Fig. 8 in the respective size ranges. Data from the measurements presented here were also mathematically fitted to a power law. The resulting equations are given in Fig. 8. It can be seen that the experimental data from this study compare very well with the data from Jung and Kittelson, concerning both the exponent as well as the coefficient of the power law. The exponent, which mainly describes the physics behind the charging process, is furthermore identical in the present data and the TSI data sheet.

In the second step, the upstream pressure was reduced by approximately 6 kPa using a capillary to mimic the pressure drop of the preseparator. The average number of elementary charges per particle was measured as described above with size classified monodisperse NaCl particles with diameters of 50, 100, 150, and 200 nm. 246 nm particles were produced from a PSL suspension. Results are also shown in Fig. 8. Even though the capillary may have introduced particle losses, these did not play a role here, because particle number concentration and current were

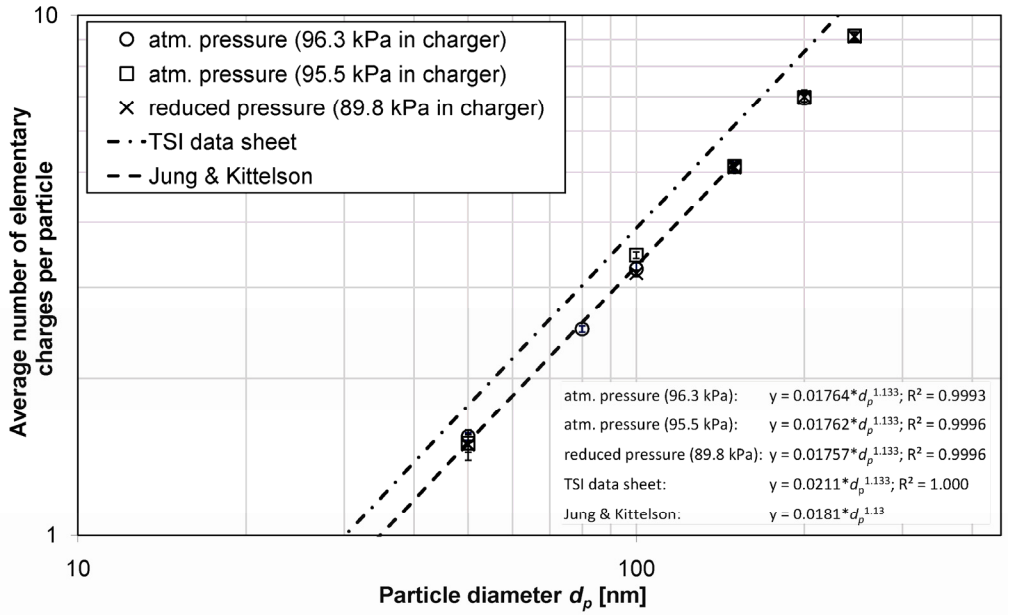

Fig. 8. Average number of elementary charges per particle as a function of particle diameter from the present study at atmospheric and reduced pressure, TSI data sheet (2004) and a publication by Jung and Kittelson (2005).

both measured downstream of the charger and the ratio was hence not affected by losses. Fig. 8 shows that all data points fall on one line, independent of the pressure inside the charger. The measured data could be fitted to a power law that is given in the figure, with a regression coefficient $R^2 > 0.999$. The exponents remain identical. The coefficients slightly differ, however only by approximately 0.3%, which certainly falls within the measurement uncertainty. A significant influence of the pressure drop on the charger was hence not detected. This confirms the assumption that the pressure reduction caused by the preseparator does not noticeably affect the charging efficiency.

SUMMARY

For unbiased measurements of nanoparticle exposure with instruments that use unipolar charging and electrometer detection, a preseparator with a defined, sharp cut off at the upper end of the nanometer size range and a pressure drop so small that it does not affect the signal of the electrical sensor is needed. A novel combination of a small cyclone with a built in virtual impactor was designed and optimized using an empirical approach. The performance of the preseparator was tested with polydisperse $BaSO_4$ and monodisperse PSL particles. For four inlet nozzle diameters from 0.70 mm to 1.20 mm, a total flow of 2.5 litres per minute and a minor virtual impactor flow of 1 litre per minute, cut-off diameters ($d_{p,50}$) varied between 220 nm and 490 nm. Compared to operation of the cyclone only, the $d_{p,50}$ was significantly reduced (e.g. from 8.1 kPa at d_{50} = 451 nm to 5.5 kPa at d_{50} = 439 nm). Comparison measurements of the mean charge per particle at different sizes using the diffusion charger of the NSAM demonstrated that a pressure reduction of 6 kPa caused by the preseparator does not noticeably affect the charging efficiency.

ACKNOWLEDGEMENT

The research leading to these results has received partial funding from TSI Inc, Shoreview, MN and the European Community's Seventh Framework Programme (FP7/2007-2013) under grant agreement n 211464-2 (NANODEVICE). Financial and technical support is gratefully acknowledged.

BIBLIOGRAPHY

Asbach, C., Fissan, H., Stahlmecke, B., Kuhlbusch, T.A.J. and Pui, D.Y.H. (2009). Conceptual Limitations and Extensions of Lung-deposited Nanoparticle Surface Area Monitor (NSAM). *J. Nanopart. Res.* 11: 101–109.

Borm, P.J.A., Robbins, D., Haubold, S., Kuhlbusch, T.A.J., Fissan, H., Donaldson, K., Schins, R., Stone, V., Kreyling, W., Lademann, J., Krutmann, J., Warheit, D. and Oberdörster, E. (2006). The Potential Risk of Nanomaterials: A Review Carried out for ECETOC. *Part Fibre Toxicol.* 3: 11.

Chan, T. and Lippmann, M. (1977). Particle Collection Efficiencies of Air Sampling Cyclones: An Empirical Theory. *Environ. Sci. Technol.* 11: 377–382.

Chen, B., Yeh, H.C. and Cheng, Y.S. (1985). A Novel Virtual Impactor: Calibration and Use. *J. Aerosol Sci.* 16: 343–354.

Fierz, M., Houle, C., Steigmeier, P. and Burtscher, H. (2011). Design, Calibration, and Field Performance of a Miniature Diffusion Size Classifier. *Aerosol Sci. Technol.* 45: 1–10.

Fierz, M., Scherrer, L. and Burtscher, H. (2002). Real-time Measurement Ofaerosol Size Distributions with an Electrical Diffusion Battery. *J. Aerosol Sci*. 33: 1049–1060.

Fissan, H., Helsper, C. and Thielen, H.J. (1983). Determination of Particle Size Distribution by Means of an Electrostatic Classifier. *J. Aerosol Sci.* 14: 354–357

Fissan, H., Neumann, S., Trampe, A., Pui, D.Y.H. and Shin, W.G. (2007). Rationale and Principle of an Instrument Measuring Lung Deposited Nanoparticle Surface Area. *J. Nanopart. Res*. 9: 53–59.

Fuchs, N.A. (1963). On the Stationary Charge Distribution on Aerosol Particles in a Bipolar Ionic Atmosphere. *Geofis. Pura Appl.* 56: 185–193.

Hernandez-Sierra, A., Alguacil, F.J. and Alonso, M. (2003). Unipolar Charging of Nanometer Aerosol Particles in a Corona ionizer. *J. Aerosol Sci.* 34: 733–745.

Hinds, W.C. (1999). *Aerosol Technology: Properties, Behavior, and Measurement of Airborne Particles,* John Wiley & Sons, New York.

Hoppel, W.A. (1978). Determination of the Aerosol Size Distribution from the Mobility Distribution of the Charged Fractions of Aerosols. *J. Aerosol Sci*. 9: 41–54.

Jung, H. and Kittelson, D.B. (2005). Characterization of Aerosol Surface Instruments in Transition Regime. *Aerosol Sci. Technol.* 39: 902–911.

Kenny, L.C. and Gussman, R.A. (1997). Characterization and Modeling of a Family of Cyclone Aerosol Preseparators. *J. Aerosol Sci.* 28: 677–688.

Kenny, L.C. and Gussman, R.A. (2000). A direct Approach to the Design of Cyclones for Aerosol-Monitoring Applications. *J. Aerosol Sci.* 31: 1407–1420.

Lapple, C.E. (1951). Processes Use Many Collector Types. *Chem. Eng.* 58: 144–151.

Leith, D. and Mehta, D. (1973). Cyclone Performance and Design. *Atmos. Environ.* 7: 527–549.

Liebhaber, F.B., Lehtimäki, M. and Willeke, K. (1991). Low-cost Virtual Impactor for Large-particle Amplification in Optical Particle Counters. *Aerosol Sci. Technol.* 15:208–213

Marple, V. (1980). Virtual Impactors: A Theoretical Study. *Environ. Sci. Technol.* 14: 976–985.

Marra, J., Voetz, M. and Kiesling, K.H. (2010). Monitor for Detecting and Assessing Exposure to Airborne Nanoparticles. *J. Nanopart. Res.* 12: 21–37.

Medved, A., Dorman, F., Kaufman, S.L. and Pöcher, A. (2000). A New Corona-based Charger for Aerosol Particles. *J. Aerosol Sci.* 31: S616–S617.

Mueller, N.C. and Nowack, B. (2008). Exposure Modeling of Engineered Nanoparticles in the Environment. *Environ. Sci. Technol.* 42: 4447–4453.

Oberdörster, G. (2010). Safety Assessment for Nanotechnology and Nanomedicine: Concepts of Nanotoxicology. *J. Internal Med.* 267:89–105

Park, D., An, M. and Hwang, J. (2007). Development and Performance Test of a Unipolar Diffusion Charger for Real-time Measurements of Submicron Aerosol Particles Having a Log-normal Size Distribution. *J. Aerosol Sci.* 38: 420–430.

Qi, C., Chen, D.R. and Pui, D.Y.H. (2007). Experimental Dtudy of a New Corona-based Unipolar Aerosol Charger. *J. Aerosol Sci.* 38: 775–792.

Savolainen, K., Alenius, H., Norppa, H., Pylkkänen, L., Tuomi, T. and Kasper, G. (2010). Risk Assessment of Engineered Nanomaterials and Nanotechnologies—A Review. *Toxicology* 269: 92–104.

Shin, W.G., Pui, D.Y.H., Fissan, H., Neumann, S. and Trampe, A. (2007). Calibration and Numerical Simulation of Nanoparticle Surface Area Monitor (TSI model 3550 NSAM). *J. Nanopart. Res.* 9: 61–69.

Sioutas, C., Koutrakis, P. and Olson, B.A. (1994). Development and Evaluation of a Low Cutpoint Virtual Impactor. *Aerosol Sci. Technol.* 21: 223–235.

Som, C., Berges, M., Chaudhry, Q., Dusinska, M., Fernandes, T.F., Olsen, S.I. and Nowack, B. (2010). The Importance of Life Cycle Concepts for the Development of Safe Nanoproducts. *Toxicology* 269: 160–169.

TSI Model 3070A Electrical Aerosol Detector Data Sheet, Available online at http://www.tsi.com/uploadedFiles/Product_Information/Literature/Spec_Sheets/3070A.pdf

Warheit, D.B., Sayes, C.M., Reed, K.L. and Swain, K.A. (2008). Health Effects Related to Nanoparticle Exposures: Environmental, Health and Safety Considerations for Assessing Hazards and Risks. *Pharmacol. Ther.* 120: 35–42.

Wilson, W.E., Stanek, J., Han, R.; Johnson, T., Sakurai, H., Pui, D.Y.H., Turner, J., Chen, D.R. and Duthie, S. (2007). Use of an Electrical Aerosol Detector as an Indicator of the Surface Area of Fine Particles Deposited in the Lung. *J. Air Waste Manage. Assoc.* 57: 211–220.

Received for review, May 5, 2011
Accepted, July 7, 2011